**Radboud Repository**

Radboud University Nijmegen

# PDF hosted at the Radboud Repository of the Radboud University Nijmegen

The following full text is a publisher's version.

For additional information about this publication click this link.
http://hdl.handle.net/2066/155376

Research Article    Open Access

# Glycolytic Metabolism is Differentially Coupled to Proliferative Potential and Morphodynamic Capacity in RAW 264.7 and Mafb/C-Maf Deficient Macrophage Lineages

Gerda Venter[1], Mietske Wijers[1], Frank TJJ Oerlemans[1], Ganesh Manjeri[2], Jack AM Fransen[1] and Bé Wieringa[1*]

[1]Department of Cell Biology, Radboud Institute for Molecular Life Sciences, Radboud University Medical Centre, Nijmegen, The Netherlands

[2]Department of Biochemistry, Radboud Institute for Molecular Life Sciences, Radboud University Medical Centre, Nijmegen, The Netherlands

*Corresponding author: Wieringa B, Department of Cell Biology, Radboud Institute for Molecular Life Sciences, Radboud University Medical Centre, P.O. 9101, 6500 HB Nijmegen, The Netherlands, Tel: +31-24-3614287; Fax: +31-24-3610909; E-mail: Be.Wieringa@radboudumc.nl

## Abstract

Background: Macrophages are highly specialized immune cells of different developmental origin, which occur in a continuum of diverse functional states in almost all tissues. In order to fulfil their complex role in tissue homeostasis and defence against pathogens they must be able to live with heterogeneous extrinsic nutrient conditions in tissue niches and handle variation in intrinsic metabolic demand that is determined by differentiation state, functional specialization and immune challenge. The purpose of the present study was to gain more insight in how metabolic specialization and versatility in fate and immune effector function of macrophages are coupled.

Methods: *In vitro* phenotypic characteristics of two macrophage cell lineages of profoundly different developmental origin and polarization capacity, RAW 264.7 and Maf-DKO cells, were analysed. By use of biochemical and cell biological approaches and scanning electron microscopy, we studied the metabolic profiles of these two types of macrophages in relation to proliferative capacity, morphological appearance of cell surface and cell shape, and phagocytic activity as index of morphodynamic potential.

Results: Comparison of gross features of carbohydrate metabolism, including levels of glycolytic enzymes Hexokinase (HK), Pyruvate Kinase (PK-M2), lactate dehydrogenase and nicotinamide phosphoribosyltransferase (Nampt), glucose and oxygen consumption and lactate production rates, and intracellular concentrations and redox ratios of NAD(P)(H) demonstrated that RAW 264.7 and Maf-DKO cells are conspicuously similar in that they both rely heavily on the use of glycolysis. In this respect they share many characteristics with primary macrophages. Strikingly, this uniform metabolic signature does not translate in behavioral-functional similarities as RAW 264.7 cells have a significantly higher proliferation rate, whereas Maf-DKO cells appear to be morphodynamically more active, form significantly more surface membrane protrusions and phagocytose complement opsonized particles much more efficiently.

Conclusion: We conclude that the global rate of glycolysis in intermediary carbohydrate metabolism is similar for the two cell lineages, but that they can make differential use of this important pathway, either to fuel high morphodynamic activity in Maf-DKO cells, or for the sustenance of cell growth in fast proliferating RAW 264.7 cells. Our findings are in keeping with the idea that macrophages may uniformly prefer use of the rapid response time of glycolysis because this pathway provides them with the ability to meet any possible short-timescale energy demand required for immune function.

## Introduction

Macrophages are highly versatile immune cells that provide a first line of defence against pathogens and help to maintain tissue homeostasis by eliminating foreign matter and apoptotic cells via phagocytosis and secreting cytokines and growth factors. They are present throughout the vertebrate body in almost all tissues, including tumors, where they can undergo region-specific differentiation [1-3]. Although all types of macrophages were originally collectively classified under the Mononuclear Phagocyte System (MPS) [4], we now know that they are in fact rather heterogeneous populations of cells, which develop from common Haematopoietic Stem Cells (HSCs) in the bone marrow or from embryonic progenitors that are already prenatally established in various tissues [5,6].

Macrophages constantly survey their environment for signs of tissue injury, dying cells, toxic materials, or invading organisms [1]. When they encounter foreign material (e.g. bacterial products) or are exposed to stimuli like inflammatory cytokines (IFN-γ, TNF, or interleukins) and Immunoglobulin G (IgG) immune complexes they gain specific functional properties and become specialized polarized cells [7], known as classically activated (M1), alternatively activated (M2 or M2a) or regulatory macrophages (M2b&c) [8-10]. After differentiation, macrophages retain plasticity and further adapt their functional phenotype in response to micro environmental cues [11], resulting in a continuum of diverse functional states [7].

Until recently, not many workers in the field of immunology paid attention to the metabolic routes and needs of specialist macrophages. Previous studies performed on mixtures of cells with different origins and activation/polarization status, like Thioglycollate-Elicited Mouse Peritoneal Macrophages (TEPMs) with a M2-like phenotype [12,13], resident peritoneal macrophages [14], or blood monocytes during differentiation [15] *in vitro* [16] under different conditions [17,18], have reported that all macrophages, irrespective of origin, tissue type, or oxygenation levels, exhibit a high rate of glycolysis. In activated macrophages up to 95% of all glucose consumed can be converted to lactate [15] instead of being oxidized via the TCA-cycle and OXPHOS, even under aerobic conditions. In this regard, macrophage metabolism closely resembles the "Warburg phenotype" of cancer cells [19,20].

New work has now revealed that this metabolic signature is not static and that differentiation and specialization can strongly influence macrophage metabolism [21]. Also the reciprocal relationship, i.e. that metabolism determines differentiation state may be true [22]. Upon polarization, carbohydrate catabolism is thus thought as being tuned to meet the specific requirements for performing different effector functions such as phagocytosis, cytokine secretion, ROS production, and ECM synthesis [21].

Unfortunately, detailed monitoring of this metabolic versatility in the in vivo situation is still not feasible, because natural macrophage populations are heterogeneous and display multiple stages of functional activation while stationary residing in their own (micro) environment or dynamically traversing tissue regions under different oxygenation and nutrient supply conditions. Moreover, metabolic studies on single cells are currently virtually impossible. The best approach for analysis and interpretation of metabolic data is therefore in vivo study of large populations of macrophages. Although relatively pure collections of primary murine macrophages can be obtained fairly easily from the peritoneal cavity, the lungs, or the bone marrow [23], these macrophages, like most mature differentiated cells, are difficult to manipulate and can be maintained in culture for only a few days [24]. Use of immortal clonally-derived macrophage cell lineages, such as the murine J744.A or RAW 264.7 monocyte/macrophage cell lines or human THP-1 cells offers an often used alternative route, however, here a caveat is that all these models have a cancerous background (i.e. originate from reticulum cell sarcoma/plasmacytoma, Abelson MLV-induced ascites or monocytic leukaemia progenitors) and possess abnormal differentiation potential [25,26]. Although there is no doubt that these macrophage lineages share many properties with primary macrophages, one must keep in mind that they also share the hallmarks of true cancer cells.

For a better understanding of metabolic versatility of macrophages comparative study of oncogenically transformed and non-transformed lineages is therefore warranted. Here we report on the parallel analysis of RAW 264.7 cells, the most intensely studied mammalian macrophage lineage, and Maf-DKO (DKO=Double Knockout) cells, a relatively novel lineage that was recently derived from mice with a MafB/c-Maf deficient hematopoietic system [27]. In the presence of M-CSF, these Maf-DKO monocytic cells proliferate and differentiate into macrophages, which can be expanded in culture without losing their differentiated phenotype. In contrast to RAW 264.7 cells, Maf-DKO cells do not have a cancerous background, show normal homing and functional integration into macrophage populations of tissues and do not themselves produce tumors when transplanted back in vivo, into mice [27]. Despite the lack of MafB and c-Maf transcription factors, this cell model is positive for specific monocyte/macrophage surface markers, and is surprisingly similar to primary macrophages with regard to gene expression profile, morphology, and phagocytic capacity [27].

We report that RAW 264.7 cells have a markedly increased proliferation rate compared to Maf-DKO cells, both in presence and absence of M-CSF. Moreover, these two macrophage cell lineages also have dramatically different morphological appearance before and after polarization and also have different phagocytosis capacity. Conspicuously, their metabolic signatures showed no dramatic differences. Both cell lineages are similarly glycolytic, with comparable responses to metabolic inhibitors, although slight differences in intracellular concentrations of NAD(H)/NADP(H) and expression levels of some glycolytic and $NAD^+$-synthesis enzymes do occur. Our findings provide the first indication that metabolic profiles of different types of macrophages may show remarkable phenotypic identity, while proliferative and immune capacity may vary widely.

## Materials and Methods

### Reagents

All reagents were obtained from Sigma-Aldrich (St. Louis, MO, USA), unless stated otherwise.

### Cell culture

RAW 264.7 cells (kind gift from Dr. Hong-Hee Kim, Department of Cell and Developmental Biology, School of Dentistry, Seoul National University, Korea [28]) were maintained in high-glucose DMEM (Gibco, Life Technologies, Paisley, UK) supplemented with 10% heat inactivated FBS (PAA laboratories, Pasching, Austria), 1 mM sodium pyruvate, and 4 mM GlutaMAX (Gibco, Life Technologies, Paisley, UK), at 37°C in a humidified atmosphere with 7.5% $CO_2$. Maf-DKO cells (kind gift from Dr. Michael H. Sieweke, Centre d'Immunologie de Marseille-Luminy (CIML), Université Aix-Marseille, France [27]) were maintained in the same way except that medium was supplemented with 20% Conditioned Medium (CM) from Macrophage Colony Stimulating Factor (M-CSF)-producing L929-cells [29].

### Proliferation assay

Cell proliferation was analyzed by sulforhodamine B (SRB) staining of protein content according to the protocol developed by Skehan et al. [30]. To compare proliferation in the presence and absence of M-CSF, RAW 264.7 and Maf-DKO cells were seeded in three 96-well plates (25,000 cells/well) in 100 μl culture medium with or without 20% L929-cell CM and incubated at 37°C. After 6 (T0), 21 (T15), and 30 (T24) hours the plates were washed twice with cold PBS and fixed with 10% trichloroacetic acid (TCA; J.T.Baker, Deventer, Holland) for 1 hour at 4°C. After fixation, plates were washed five times with water and stored at -20°C until all plates were collected. Cellular protein was stained with 50 μl 0.5% SRB in 1% acetic acid for 20 minutes after which wells were washed four times with 1% acetic acid. Plates were dried at 60°C for 3 hours, protein was dissolved in 150 μl 10 mM Tris-HCl (pH 10.5), and the absorbance of each well was measured at 510 nm on a BioRad Benchmark Plus micro plate reader. Values were corrected for background SRB staining by subtracting the average absorbance value of wells that contained medium only, from that of wells with cells. To determine the effect of 2-DG and oligomycin on proliferation, RAW 264.7 and Maf-DKO cells were seeded in three 96

well plates at a density of 7,500 and 25,000 cells/well, respectively. RAW 264.7 cells were incubated for 6 hours and Maf-DKO cells overnight before wells were washed once with medium containing either 10 mM 2-deoxy-D-glucose (2-DG) or 2.5 μM oligomycin and cells were incubated in the same medium for 24, 48 or 72 hours. Cells were then fixed and stained as described above.

## Western blot analysis

Protein expression was analysed by western blot analysis. After washing cells twice with cold PBS in 6 cm culture dishes, cell lysates were prepared in lysis buffer (50 mM Tris-HCl pH 7.5, 100 mM NaCl, 5 mM $MgCl_2$, and 0.5% NP-40; 4°C) and stored at -20°C until analysis. Lysates containing ± 10 μg protein were mixed with 5x sample buffer (0.25 % Bromophenol Blue, 0.5 M DTT, 50 ml glycerol, 10 %SDS, and 0.25 M Tris-HCl pH 6.8), heated at 95°C for 5 minutes, and loaded onto 10 or 12% SDS-PAGE gels, depending on the size of the protein of interest. After electrophoretic separation, proteins were blotted onto PVDF membranes. Membranes were blocked with 5% (w/v) skimmed milk in PBS-T (HXK1, HXK2, LDH-A, actin and NAMPT) or TBS-T (PKM2 and NAPRT) for 1 hour and labelled overnight with a mouse anti-Tubulin (1:5000; DSHB, University of Iowa) and either a goat anti-HXK1 (1:200; Santa Cruz Biotechnology), goat anti-HXK2 (1:200; Santa Cruz Biotechnology), goat anti-LDH-A (1:5000; Cell Signalling Technology), rabbit anti-PKM2 (1:1000; Cell Signalling Technology), rabbit anti-actin (1:1000; Cytoskeleton Inc.), rabbit anti-NAMPT (1:2500; Behthyl Laboratories, Montgomery, TX, USA) or anti-NAPRT (1:1000; Sigma-Aldrich, St. Louis, MO, USA) antibodies at 4°C. After washing the membranes three times for 5 minutes with PBS-T or TBS-T, they were incubated with IR Dye secondary antibodies (donkey anti-goat 680, goat anti-rabbit 680, goat anti-rabbit 800, goat anti-mouse 680, and/or goat anti-mouse 800) for one hour at room temperature. This was followed by 4 wash steps of 5 minutes each in PBS-T or TBS-T, a final wash step in PBS, and signal detection on the Odyssey Infrared Imaging System (LI-COR Biosciences, Lincoln, NE, USA). Tubulin served as loading control and reference for calculation of protein content.

## Glucose and lactate measurements

Glucose consumption measurements were based on the Amplex Red Glucose/Glucose Oxidase assay kit from Molecular probes (Life Technologies, Eugene, Oregon, USA). Glucose, glucose oxidase, and Amplex Red reagent were used from the kit but horseradish peroxidase was obtained from Sigma-Aldrich (St. Louis, MO, USA) and 1x reaction buffer was replaced with 0.05 M Tris-HCl, pH 7.5. Apart from these minor changes, the kit protocol was followed as described by the manufacturer. Lactate production was measured using the same protocol as for glucose consumption but replacing glucose oxidase with lactate oxidase and including a lactate standard series instead of glucose. Cells were seeded in 12 well tissue culture plates in medium containing 20% L929-cell CM and incubated overnight. For glucose measurements, medium containing 5 mM glucose was used while lactate production was measured for cells grown in 25 mM glucose medium. The next day, wells were rinsed with pure DMEM containing no glucose and fresh control medium (containing 10% heat inactivated dialyzed FBS, 1 mM sodium pyruvate, and 4 mM GlutaMAX) or medium containing 2.5 μM oligomycin was added. After 6 hours, medium was collected and supernatants were snap frozen in liquid nitrogen and stored at -20°C until analysis. Cytosolic extracts were prepared in lysis buffer (50 mM

Tris-HCl pH 7.5, 100 mM NaCl, 5 mM $MgCl_2$, and 0.5% NP-40; 4°C) and total protein was determined with the Bradford assay. Glucose consumption was calculated by subtracting the amount of glucose in the sample from that in medium without cells. Lactate production was calculated by subtracting the concentration of any lactate in the medium without cells from that of the samples. Glucose and lactate assays were performed in parallel.

## LDH-isoenzyme expression

LDH-isoenzymes were separated using the SAS-MX LDH Isoenzyme gel electrophoresis test from Helena Biosciences Europe, according to the manufacturer's specifications. Cell lysates were prepared as for western blot and protein concentration was determined with the Bradford assay. Per lane, approximately 2.8 μg of protein was loaded.

## NAD(H)/NADP(H) measurements

Intracellular $NAD^+$, NADH, $NADP^+$, NADPH concentrations were measured exactly as described [31].

## Oxygen consumption measurements

An Oroboros Oxygraph-2k respirometer was used to measure oxygen consumption in RAW 264.7 and Maf-DKO cells according to a standard protocol provided by the manufacturer. RAW 264.7 cells were incubated in medium with 20% L929-cell CM for at least 24 hours prior to assay. The two cell lines were analysed in parallel in two separate chambers of the respirometer. After air calibration of the medium in the chambers and stabilization of the signal, 1 x 106 cells (in 60 μl medium) were injected into the respective chambers. Basal respiration rate was measured at the point where the $O_2$-flux signal stabilized. Oligomycin (2.5 μM) was added to each chamber and the leak respiration rate was determined after stabilization of the signal. Next, 7 μM carbonyl cyanide-p-trifluoromethoxyphenylhydrazone (FCCP, a mitochondrial uncoupler) was added to reach maximal oxygen consumption in the cells. Finally, 30 nM rotenone was added and after stabilization of the system, the residual oxygen consumption could be determined. The data was analysed using the DatLab software provided with the instrument.

## Scanning electron microscopy

RAW 264.7 and Maf-DKO cells were seeded on 12 mm glass coverslips in 24-well plates in medium with or without L929-cell CM and activated with 100 ng/ml LPS or left non-activated. Cells were washed once with PBS and fixed with 2% glutaraldehyde in 0.1 M sodium cacodylate buffer for 1 hour. After washing cells twice with sodium cacodylate buffer, coverslips were stored in the same buffer at 4°C until further fixation with 1% $OsO_4$ (osmium tetroxide) for 30 minutes. Coverslips were then washed once with water and dehydrated in a graded series of alcohol, critical point dried, and mounted for scanning electron microscopy (JEOL SEM6340F Field Emission Scanning Electron microscope). Images were acquired at 500x as well as a 2000x magnification.

## Quantification of surface membrane protrusions

Dorsal surface protrusions were quantified using SEM-images. A region of interest with an area of 20-130 $μm^2$ was drawn on the cell body of single cells using Fiji imaging software. All protrusive

structures within this region were counted and the number of surface protrusions per square micron was calculated. RAW 264.7 (n=17) and Maf-DKO (n=25) cells from five different fields were analysed.

## Cellular actin staining

RAW 264.7 and Maf-DKO cells were seeded on 12 mm glass coverslips in 24-well plates in medium with or without L929-cell CM and activated with 100 ng/ml LPS or left non-activated. Cells were washed twice with PBS and fixed in 2% paraformaldehyde in 0.2 M sodium phosphate buffer for 30 minutes. After washing twice with PBS and twice with PBS containing 20 mM glycine (MP Biomedicals, Illkirch Cedex, France; PBS-G) cells were permeabilized with 0.1% saponine/PBS-G for 20 minutes. This was followed by actin staining with Alexa 568-labeled phalloidin (1:600 in 0.1% saponine/PBS-G) for 1 hour. Cells were successively washed four times for 2-4 minutes with 0.1% saponine/PBS-G and once with PBS alone. Coverslips were removed from wells, rinsed once in water, air dried, and embedded in MoWiol on microscope slides. Images were acquired on a Zeiss LSM510 META confocal laser scanning microscope using a 63x objective and processed using Fiji imaging software.

## Phagocytosis assay

Phagocytic activity was determined as zymosan ingestion capacity essentially as described by Chang, et al. [28]. Zymosan particles were dissolved in PBS at 10 mg/ml and left to rehydrate for at least one hour. Next, zymosan was sonicated three times for 5 seconds, spun down, resuspended in carbonate buffer (pH 9.6), sonicated, and incubated with 1 µg/ml Fluorescein Isothiocyanate (FITC) for 1 hour at room temperature, in the dark. After FITC labeling, zymosan was washed three times with carbonate buffer and incubated in 1 M Tris-HCl, pH 8.0, for 30 minutes. Zymosan was then washed twice with PBS and finally resuspended in PBS. After one more sonication step, FITC-labeled zymosan was divided in aliquots, frozen in liquid nitrogen, and stored at -20°C.

For phagocytosis assays without M-CSF, 100,000 RAW 264.7 cells were seeded per well in normal culture medium and 200,000 Maf-DKO cells per well in medium with 20% L929-cell CM. For assays with M-CSF, both RAW 264.7 and Maf-DKO cells were seeded in medium containing L929-cell CM at a density of 75,000 and 200,000 cells per well, respectively. Where applicable, cells were pre-incubated in medium containing 2.5 µM oligomycin (0 or 24 hours) or 10 mM 2-DG (3 hours) and activated overnight with 100 ng/ml LPS. FITC-labelled zymosan particles were complement opsonized by incubation in foetal bovine serum for 1 hour at 37°C, washed twice with PBS, and finally resuspended in serum-free medium with or without L929-cell CM and, where applicable, with or without oligomycin and 2-DG. Cells were washed once with serum-free medium and incubated with 1 ml zymosan suspension for 30 minutes at 37°C. The particle-to-cell ratio was approximately 10:1. Particle engulfment was terminated by washing cells twice with PBS and removing extracellular zymosan by treatment with 500 µl 100 U/ml lyticase for 10 minutes at room temperature. Successively, cells were detached with 0.05% trypsin/0.5 mM EDTA (Gibco, Life Technologies, Paisley, UK), resuspended in 1 ml medium with serum, pelleted, and finally resuspended in 200 µl 1% paraformaldehyde in PBS. Samples were analyzed by FACS and phagocytosis efficiency was determined by measuring the fluorescence intensity of the FITC positive population as well as the percentage of cells in that population. The phagocytic index of each sample was

calculated as the product of the mean FITC intensity of the positive population times the % of FITC positive cells.

## Statistical analysis

Data was analyzed either with the Student's t-test or using a two-way ANOVA and the Bonferroni post-test (GraphPad software, Inc., Version 4). Values are expressed as mean ± SEM. Values were considered to be significantly different when p values were < 0.05.

## Results and Discussion

### RAW 264.7 and Maf-DKO proliferation in the presence of M-CSF

Cell proliferation is essential for innate immunity, required for development and maintenance of tissue resident macrophages [6]. To better compare the potential coupling between metabolic phenotype and proliferative capacity of RAW 264.7 and Maf-DKO cells in culture, we analysed first the effects of absence or presence of M-CSF (in conditioned medium from L929 cells) on cell proliferation. In vivo, M-CSF after being secreted by various cells [32,33], is found in the circulation [34], from where it stimulates proliferation via activation of cell cycle genes. M-CSF is also a known modulator of metabolic activities [35]. Of note, MafB/c-Maf deficient (Maf-DKO) monocytes require macrophage colony stimulating factor (M-CSF or CSF-1) for their in vitro differentiation into M2-macrophages [27]. For RAW 264.7 cells to achieve differentiation in vitro, continuous presence of M-CSF is no prerequisite, although they do require additional stimulus to obtain either an M1 or M2 polarization state.
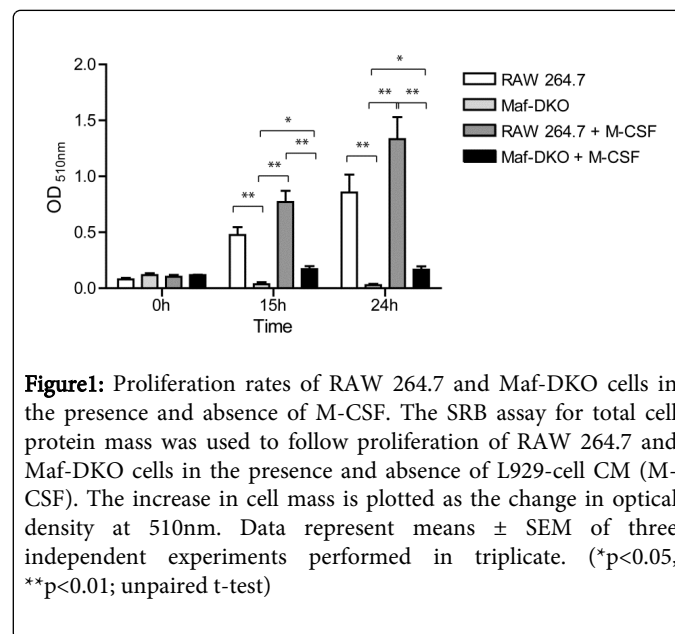


**Figure 1:** Proliferation rates of RAW 264.7 and Maf-DKO cells in the presence and absence of M-CSF. The SRB assay for total cell protein mass was used to follow proliferation of RAW 264.7 and Maf-DKO cells in the presence and absence of L929-cell CM (M-CSF). The increase in cell mass is plotted as the change in optical density at 510nm. Data represent means ± SEM of three independent experiments performed in triplicate. (*p<0.05, **p<0.01; unpaired t-test)

Under standard medium conditions (DMEM supplemented with FBS, pyruvate and GlutaMax but without M-CSF) RAW 264.7 cells had a significantly higher proliferation rate (Figure 1). In the presence of M-CSF, added as 20% Conditioned Medium (CM), RAW 264.7 proliferation was further increased. Maf-DKO cells, on the other hand, failed to divide without M-CSF but even in the presence of M-CSF Maf-DKO cells had a significantly slower growth rate compared to RAW 264.7. The high rate of traverse through cell cycle and the

independence of RAW 264.7 proliferation on M-CSF most likely reflect the malignant background of these cells. Conversely, the considerable slower cycle time of Maf-DKO cells and the fact that M-CSF is obligatory for their survival, confirms that these cells still have retained features that are typical for primary macrophages. Whether the double loss of MafB and c-Maf transcription factors also attributed to the growth properties of Maf-DKO cells *in vitro* is not known, but apparently this has had no large effect on their responsiveness to M-CSF (see also Martinez et al. [35]).

## Glycolytic and mitochondrial metabolism

For most cell types , especially tumor cells, proliferative capacity is tightly coupled to glucose metabolism, whereby rapid cell division is usually accompanied by an adaptive shift in metabolism to aerobic glycolysis [19]. Macrophages could, however, be special in that even in the untransformed state they appear highly glycolytic [36,37]. In order to determine and compare the extent to which cancerous RAW 264.7 and normal Maf-DKO cells depend on glycolysis or mitochondrial oxidative phosphorylation (OXPHOS), we assessed proliferation in the presence and absence of the glycolysis inhibitor 2-deoxy-D-glucose (2-DG) and the OXPHOS inhibitor oligomycin. In both cell lines glucose metabolism via glycolysis appeared to be the primary pathway to fuel proliferation. In the presence of 2-DG, proliferation ceased within 24 hours (Figures 2A and 2B). In contrast, in the presence of oligomycin, both cell lines continued to proliferate for at least 72 hours, although their growth rate was significantly reduced (Figures 2A and 2B). These results confirm that RAW 264.7 and Maf-DKO cells – in accordance with their monocyte-macrophage character - are both highly glycolytic but that mitochondrial OXPHOS capacity in both cell lineages must be intact, and used, to attain maximal growth rates.
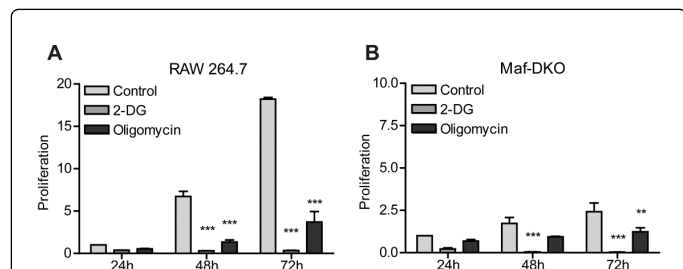


**Figure 2:** Proliferation of RAW 264.7 and Maf-DKO cells in the presence of glycolysis inhibitor 2-DG and OXPHOS inhibitor oligomycin. RAW 264.7 (A) and Maf-DKO (B) cells were incubated in control medium or medium containing 10mM 2-DG or 2.5 µM oligomycin for 24, 48, or 72 hours, after which protein content was determined with the SRB assay as described in the legend of Figure 1, and in M&M. In order to enable comparison of proliferation rates, absorbance values were normalized to the control values at 24 hours, since RAW 264.7 and Maf-DKO cells were not seeded at equal densities and absorbance values at 24 hours varied between cell lines. Data represent means ± SEM of three independent experiments performed in triplicate. (**p < 0.01, ***p < 0.001, Two-way ANOVA and Bonferroni posttest)

To compare aspects of intermediary metabolism of RAW 264.7 and Maf-DKO cells more closely, we next measured glucose consumption and lactate production, compared the expression of certain glycolytic enzymes, and determined mitochondrial respiration. Glucose consumption and lactate production were measured relative to the

amount of protein per well. No significant differences were found in the amount of glucose consumed (Figure 3A) and, although Maf-DKO cells tended to produce less lactate (Figure 3B), both cell lines showed a high glycolytic flux to lactate, with RAW 264.7 cells converting 75% and Maf-DKO cells converting 70% of all glucose to lactate (ratio of control bars, Figures 3A and 3B).
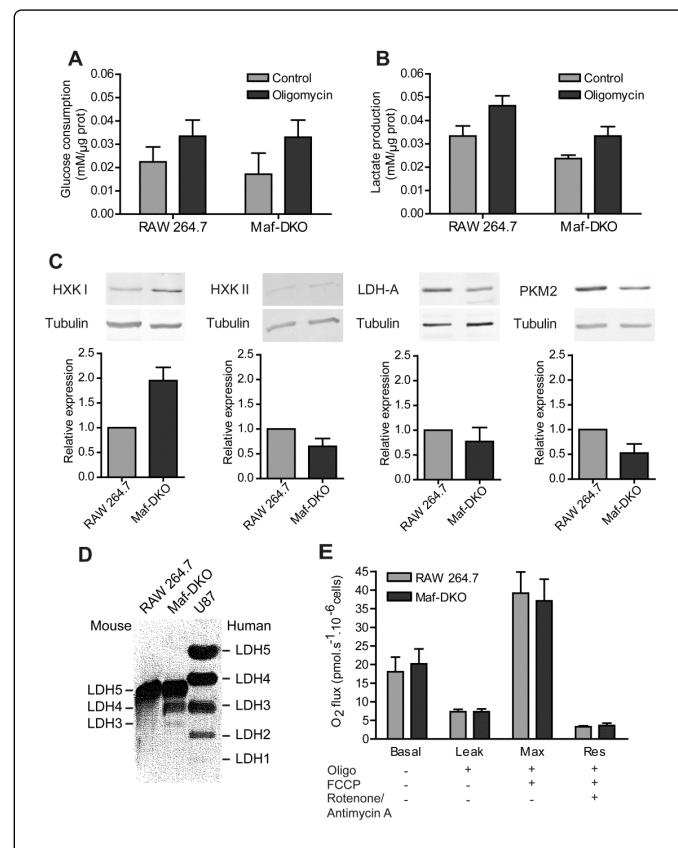


**Figure 3:** RAW 264.7 and Maf-DKO cells are highly glycolytic. Glucose consumption (A) and lactate production (B) in RAW 264.7 and Maf-DKO cells in the presence and absence of the OXPHOS inhibitor oligomycin. (C) Expression levels of four metabolic enzymes that were noticeably different between the two cell lines. Protein expression (relative to tubulin) was calculated from the band intensities of three different blots and normalized to the expression in RAW 264.7 (n=3 different assays). D, Zymogram analysis of LDH-isoenzyme expression in RAW 264.7 and Maf-DKO cells. To verify the gel's capacity to separate LDH1-LDH5 isoforms of mouse and human origin, a lysate of the human glioma cell line U87 (which expresses all five isoforms) was run in parallel as a control (according to Eyben et al. [58]). Note the presence of low levels of the LDH3 and LDH4 tetramers, containing two or one H-subunits from the LDH-B gene in the Maf-DKO lysate. E, Mitochondrial respiration measured as the basal oxygen consumption (Basal), the leak respiration (Leak), maximal oxygen consumption (Max), and residual oxygen consumption (Res). Data in (C) represent band intensities of HXK I, HXK II, LDH-A, and PKM2 of one blot, relative to tubulin. Data in A and B represent means ± SEM of three independent experiments performed in triplicate, and in E means ± SEM of four experiments performed with RAW 264.7 and Maf-DKO cells in parallel.

This percentage is lower than what was reported for quiescent peritoneal macrophages in an earlier study by Rodríguez-Prados et al. [15] where these cells converted 95% of all glucose to lactate. In the same study RAW 264.7 were shown to have a glucose-lactate-conversion of 80%, but to have an increased glycolytic flux rate (i.e. consume and produce more glucose and lactate, respectively). Maf-DKO cells, therefore, seem to have a glycolytic flux and flux rate more comparable to RAW 264.7 cells than to quiescent peritoneal macrophages under the culture conditions that we used in our analyses. In both cell lines glucose consumption and lactate production was marginally increased when mitochondrial OXPHOS was inhibited with oligomycin.

Glycolytic enzymes are often differentially regulated in cancer cells [38]. When the expression levels of some glycolytic enzymes of Raw 264.7 and Maf-DKO cells were compared on western blot, we did not observe any overt differences. We did, however, notice that the expression levels of lactate dehydrogenase (as verified by the level of the A subunit; LDH-A), and pyruvate kinase M2 (PKM2) tended to be slightly higher in RAW 264.7 cells, while the opposite was true for HXK I (Figure 3C). Again, the profiles for enzyme expression are indicative for sustenance of a high glycolytic rate, reminiscent of the metabolic signatures of true cancer cells. It is particularly noteworthy that both types of macrophages do express PKM2 (Figure 3C), the special PKM splice isoform which has a pivotal role in tuning of glycolytic rate and also use of associated biosynthetic pathways for the generation of nucleotides (i.e. via the PPPathway) and lipids in fast proliferating cells [39].

For LDH, the enzyme that catalyses the conversion of pyruvate to lactate we performed a subunit composition analysis in addition to the quantification of the main subunit, LDH-A (western blot, Figure 3C). Lactate dehydrogenase may exist in five different isoforms (LDH1-5) that differ from one another with regard to the ratio of the A and B subunits in the tetramer and the capacity for pyruvate to lactate conversion under physiological conditions. Zymogram analysis showed that Maf-DKO cells, in contrast to RAW 264.7 cells, express low amounts of LDH-B that enables the production of LDH3 and LDH4. Still, zymogram intensities revealed no other overt differences. As LDH5 activity staining appeared equally strong and this isoform was by far most dominantly expressed in both cell types (Figure 3D) we conclude that the available capacity for pyruvate and lactate interconversion does not noticeably differ between the two macrophage lineages.

When pyruvate is not converted to lactate it is transported across the mitochondrial membrane and catabolized via the TCA-cycle and used to produce ATP via OXPHOS. In order to compare the mitochondrial activity of RAW 264.7 and Maf-DKO cells, we measured oxygen consumption in absence and presence of certain OXPHOS inhibitors in order to determine basal $O_2$-consumption as well as the amount of oxygen that is consumed without producing ATP (leak), the respiration capacity (maximal respiration rate), and the amount of oxygen consumption by systems other than the electron transport chain (residual oxygen consumption), for example NADPH oxidases [40]. Both cell lines exhibited a relatively low $O_2$-consumption (~ 20 pmol.s$^{-1}$.10$^{-6}$ cells compared to ~ 100 pmol.s$^{-1}$.10$^{-6}$ cells for mouse embryonic fibroblasts [41]; Figure 3E). Indeed, if only a minor fraction of glucose-derived pyruvate enters the TCA cycle and ultimately serves to fuel OXPHOS, this may explain why treatment with oligomycin did not significantly alter the glycolytic flux (Figures 3A and 3B). Of note, no differences were detected in basal oxygen consumption between RAW 264.7 and Maf-DKO, neither did the cell lines differ in leak, maximal, or residual $O_2$-consumption (Figure 3E).

## Intracellular NAD (H) and NADP(H) levels

One crucial parameter in the regulation of flux through intermediary carbohydrate metabolism, notably at steps in the 3C stage of glycolysis (the pyruvate-to-lactate conversion) or in further breakdown via the TCA pathway in mitochondria, is the NAD$^+$/NADH redox ratio and the absolute intracellular concentration of these Pyrimidine Nucleotides (PNs). Redox ratio and absolute concentration of the other main PN pair in mammalian cells, NADP$^+$ and NADPH, is also an important but independent reporter of metabolic state, and – amongst others – an indicator of a cell's capacity to cope with oxidative stress [42].
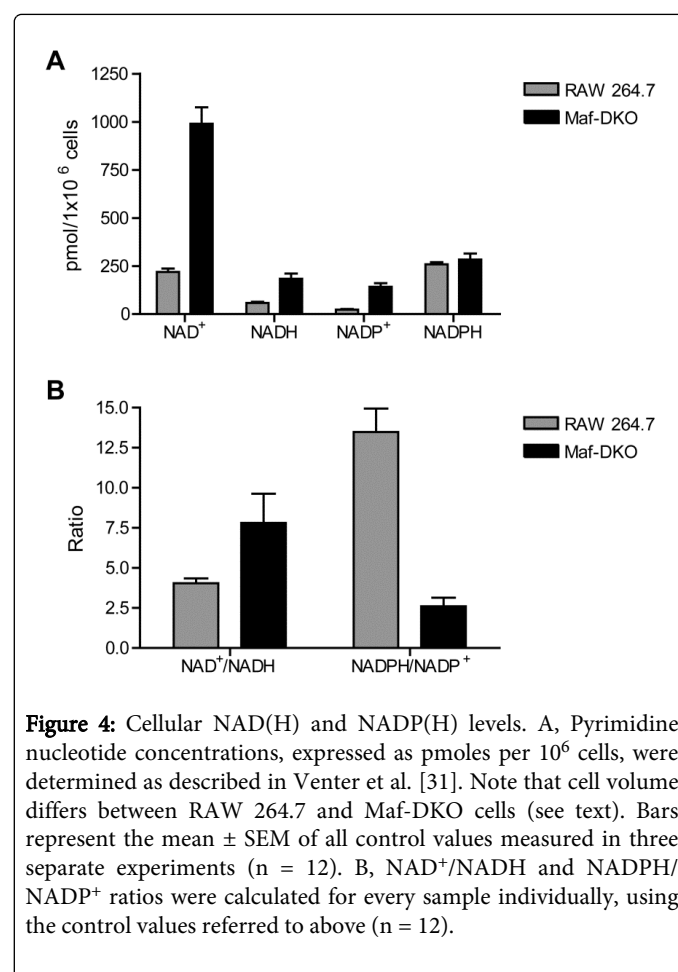


**Figure 4:** Cellular NAD(H) and NADP(H) levels. A, Pyrimidine nucleotide concentrations, expressed as pmoles per 10$^6$ cells, were determined as described in Venter et al. [31]. Note that cell volume differs between RAW 264.7 and Maf-DKO cells (see text). Bars represent the mean ± SEM of all control values measured in three separate experiments (n = 12). B, NAD$^+$/NADH and NADPH/NADP$^+$ ratios were calculated for every sample individually, using the control values referred to above (n = 12).

Direct comparison of total NAD$^+$, NADH, NADP$^+$ and NADPH concentrations measured in pools of 1 x 10⁶ RAW 264.7 and Maf-DKO cells each, revealed steady-state concentrations of 219.31 ± 17.81 pmol vs. 989.91 ± 85.63 pmol for NAD$^+$, 57.85 ± 5.99 pmol vs. 183.60 ± 27.11 pmol for NADH, 23.23 ± 3.65 pmol vs. 141.84 ± 19.07 pmol for NADP$^+$, and 258.61 ± 11.83 pmol vs. 283.50 ± 31.79 pmol for NADPH, respectively (Figure 4A). From cell shape and size differences between RAW 264.7 and Maf-DKO cells (see Figure 5 and data not shown) we estimate that Maf-DKO cells have an approximately 3-fold larger volume. Hence, we conclude that the absolute concentrations of the NAD$^+$ and NADH do not differ conspicuously between the two cell types.
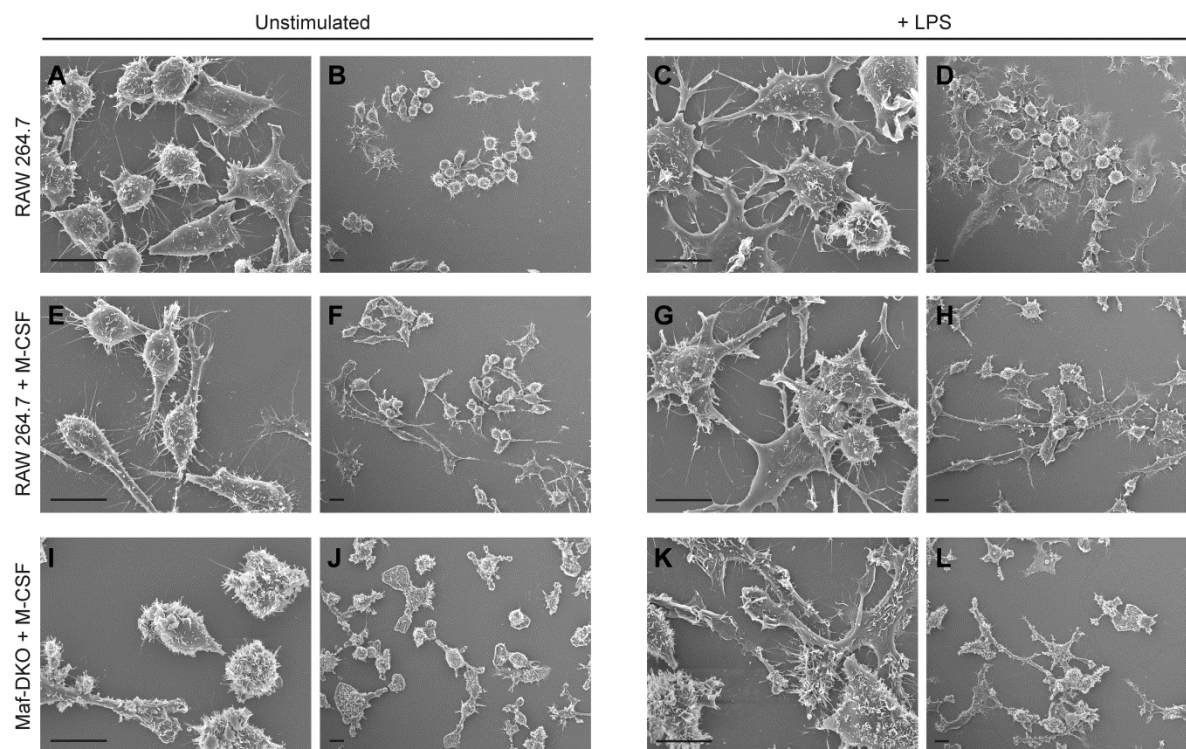
**Figure 5:** Scanning electron microscope images of RAW 264.7 and Maf-DKO cells, cultured in the presence and absence of M-CSF and LPS. RAW 264.7 cells in normal culture medium (A-D), RAW 264.7 cells in medium containing 20% L929-cell CM (E-H), Maf-DKO cells in medium containing 20% L929-cell CM (I-L). (Bars = 10 μm)

In keeping with this finding is that both cells express almost similar and clearly detectable levels of NAMPT, the key and rate limiting enzyme for salvage synthesis of $NAD^+$ (similar when normalized to total cellular protein, or 3-fold less in Maf-DKO when normalized to total tubulin as loading control; see Supplementary Figure S1 and also Venter et al. [31]).

Interestingly, however, the $NADPH/NADP^+$ redox ratio differed between cell types and appeared in RAW 264.7 cells 4-fold higher than in Maf-DKO cells (Figure 4B). This finding may be explained by assuming that RAW 264.7 cells have to cope with a higher level of oxidative stress, a common feature found in cells that have undergone malignant transformation [43,44]. Also other genome differences, including the effects of MafB/c-Maf absence in Maf-DKO cells or oncogenic changes in the RAW 264.7 genome may have played a role. A more detailed characterization of $NAD^+$-related metabolism and its coupling to macrophage immune function can be found in Venter et al. [31].

When taken together, our descriptive characterization data reveal that the signatures of carbohydrate metabolism do not overly differ between RAW 264.7 and Maf-DKO cells. RAW 264.7 may be marginally more active in pyruvate-to-lactate conversion, and invest more heavily in NADPH production (presumably via activation of the pentose phosphate pathway), but oxygen consumption rate, as a measure for mitochondrial pathway activity, was at a similar low level for both cell types.

## Morphodynamic properties of RAW 264.7 and Maf-DKO cells

In various other studies an inverse reciprocal relationship between proliferation capacity and morphological and functional specialization upon polarization has been demonstrated [45]. Also a tight coupling between intermediary metabolism and morphodynamic activity has been well established [31,42,46-48]. In view of these different types of coupling, and because no conspicuous differences in metabolic profiles were found between RAW 264.7 and Maf-DKO cells, we next asked whether our findings would also predict similarities in morphodynamic phenotype.

To answer this question we first used scanning electron microscopy to compare the morphological appearance of RAW 264.7 cells with that of Maf-DKO cells. As M-CSF induces morphology changes in macrophages [49], we tested RAW 264.7 cells under medium conditions with and without L929-cell CM, whereas Maf-DKO was continuously kept in presence of M-CSF to maintain their differentiated phenotype.

Both lineages were additionally stimulated overnight with 100 ng/ml LPS before fixation and image acquisition. Strikingly, profound differences were observed in the growth pattern and morphology of RAW 264.7 cells in the presence and absence of M-CSF. Without M-CSF, RAW 264.7 cells grew in a clump-wise fashion and had a rounded shape (Figures 5A and 5B), while the addition of M-CSF induced the formation of cellular protrusions and caused the cells to arrange themselves more loosely, similar to Maf-DKO cells (Figures

5E and 5F). Interestingly, Maf-DKO cells displayed a more complex surface morphology compared to RAW 264.7. Maf-DKO cell surfaces were densely decorated with protrusive membrane structures, which we henceforth designate as membrane ruffles throughout this piece (Figures 5I and 5J). RAW 264.7 cell surfaces were more 'bald', displaying only few ruffles (Supplementary Figure S2). LPS induces an inflammatory phenotype in macrophages that is accompanied by morphological change [50,51]. Under our culture conditions cell spreading was prominently induced by LPS in RAW 264.7 both in the absence and presence of M-CSF (Figures 5C, 5D, 5G and 5H), as well as in Maf-DKO cells (Figures 5K and 5L).

To us, the relative high abundance of ruffle-like structures on Maf-DKO cells suggests that these cells have a dynamically more active cortical actin cytoskeleton than RAW 264.7 cells. This feature could help them to effectively probe their environment. Possibly, under the conditions used, a high percentage of the "cell-dorsal" surface protrusions represent the membrane folds that are actively involved in the non-selective uptake of molecules, nutrients, and antigens from the medium through a process called macropinocytosis [9].
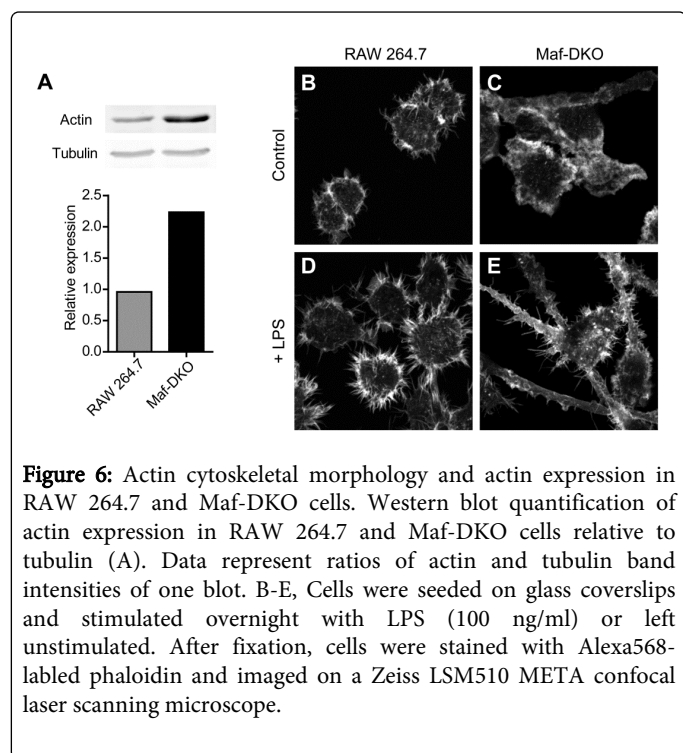


**Figure 6:** Actin cytoskeletal morphology and actin expression in RAW 264.7 and Maf-DKO cells. Western blot quantification of actin expression in RAW 264.7 and Maf-DKO cells relative to tubulin (A). Data represent ratios of actin and tubulin band intensities of one blot. B-E, Cells were seeded on glass coverslips and stimulated overnight with LPS (100 ng/ml) or left unstimulated. After fixation, cells were stained with Alexa568-labled phaloidin and imaged on a Zeiss LSM510 META confocal laser scanning microscope.

Our results thus suggest that Maf-DKO cells may be much more active in this uptake than RAW 264.7. Indeed, this interpretation would be consistent with the findings of Aziz et al. [52], who observed that the actin organization of MafB-deficient macrophages is altered and that a number of proteins involved in actin polymerization, as well as actin itself, were upregulated compared to control cells, thereby suggesting a role for MAFB in the regulation of actin dynamics. Indeed, two pieces of evidence corroborate this picture here, and suggest a differential role for actin in Maf-DKO and RAW 264.7 cells. Firstly, when normalized to tubulin expression, we found that Maf-DKO cells expressed considerably more actin than RAW 264.7 cells (Figure 6A). Secondly, staining with phalloidin revealed that RAW 264.7 and Maf-DKO cells have a noticeably different morphology of the actin cytoskeleton (Figures 6B and 6C). In RAW 264.7 cells,

prominent actin-rich filopodial structures could be distinguished, while Maf-DKO cells displayed a more 'cloudy' actin staining. This 'cloudy' staining could be the result of the dense organization of membrane sheets and ruffles on the surface of Maf-DKO cells, making it difficult to distinguish separate structures. In the presence of LPS, Maf-DKO cells also developed actin rich filopodia, but these structures were still more prominent in RAW 264.7 cells (Figures 6D and 6E).

Next, to verify whether the similarities in metabolic phenotype indeed combine with differences in actin-based morphodynamic behavior, and that not just a picture of false dichotomy is created for the two macrophage lineages on the basis of differences in static appearance, we decided to measure phagocytosis efficiency as a quantitative measure of mophodynamic activity. To this end, we determined uptake efficiency of Complement Opsonized Zymosan (COZ) in the presence and absence of LPS and M-CSF. As shown in Figure 7A, RAW 264.7 phagocytosis was low in the absence of LPS and M-CSF (-LPS). In the presence of LPS, the ability to engulf COZ was markedly improved, while the addition of M-CSF reduced the RAW 264.7 phagocytosis efficiency. Aziz, et al. [27] reported that, compared to primary wild type macrophages, the phagocytic activity of Maf-DKO cells is not altered. We found here that, compared to RAW 264.7 cells, they exhibited significantly greater phagocytosis efficiency, even in the absence of LPS or M-CSF (Figure 7A). Pre-stimulation with LPS did not affect COZ engulfment by Maf-DKO cells, while M-CSF increased the phagocytosis efficiency significantly. The two cell lines, therefore, clearly have a differential dependency on M-CSF for phagocytosis. Most literature studies report on a stimulatory effect of M-CSF on phagocytosis [53,54] in agreement with our observation for the Maf-DKO cells, although an inhibitory effect of M-CSF on phagocytosis of serum opsonized yeast cells in resident peritoneal macrophages is mentioned in one study [49]. Currently it is unclear how M-CSF can have such differential effects on phagocytosis in different macrophage cells. Although truly opposing effects are difficult to explain, it is possible that activity of the receptor for M-CSF (CSF-1R) or downstream pathways in M-CSF-induced signalling are differentially controlled in macrophages of different origin. Our observation that RAW 264.7 cells required LPS induction to activate phagocytic capacity, while Maf-DKO cells were far more efficient in phagocytosis of COZ particles even in the absence of any additional external stimulus strengthen this possibility. Another explanation may be that the difference is not in signalling pathways but that (as we show in Figures 5A and 5I) Maf-DKO cells are structurally better equipped to capture phagocytic targets than RAW 264.7 cells, because their surface is permanently more abundantly decorated with membrane sheets and ruffles, structures that have been shown to be involved in the capturing of complement opsonized particles [55]. Upon stimulation with LPS, membrane ruffle formation is induced (Figure 5C and 5D), along with the activation of the complement receptor [56], explaining why phagocytosis is improved with LPS in RAW 264.7 cells.

Finally, we analyzed whether metabolic modulation would affect morphodynamic capacity differentially, to explain the obvious qualitative and quantitative phenotypic differences between both macrophage lineages. For this, rather short-term analyses, using conditions with 3 hr or 24 hr inhibition with 2-deoxy-D-glucose (2-DG) or oligomycin, respectively, were chosen to avoid metabolic adaptation, or effects on growth or other aspects of cell viability (Figure 1). Interestingly, our tests revealed that phagocytic COZ-uptake capacity by RAW 264.7 and Maf-DKO cells decreased similarly strong when glycolysis was impaired, but that blocking of

mitochondrial oxidative phosphorylation activity [46] had no effect on both cell lines (Figures 7B and 7C).
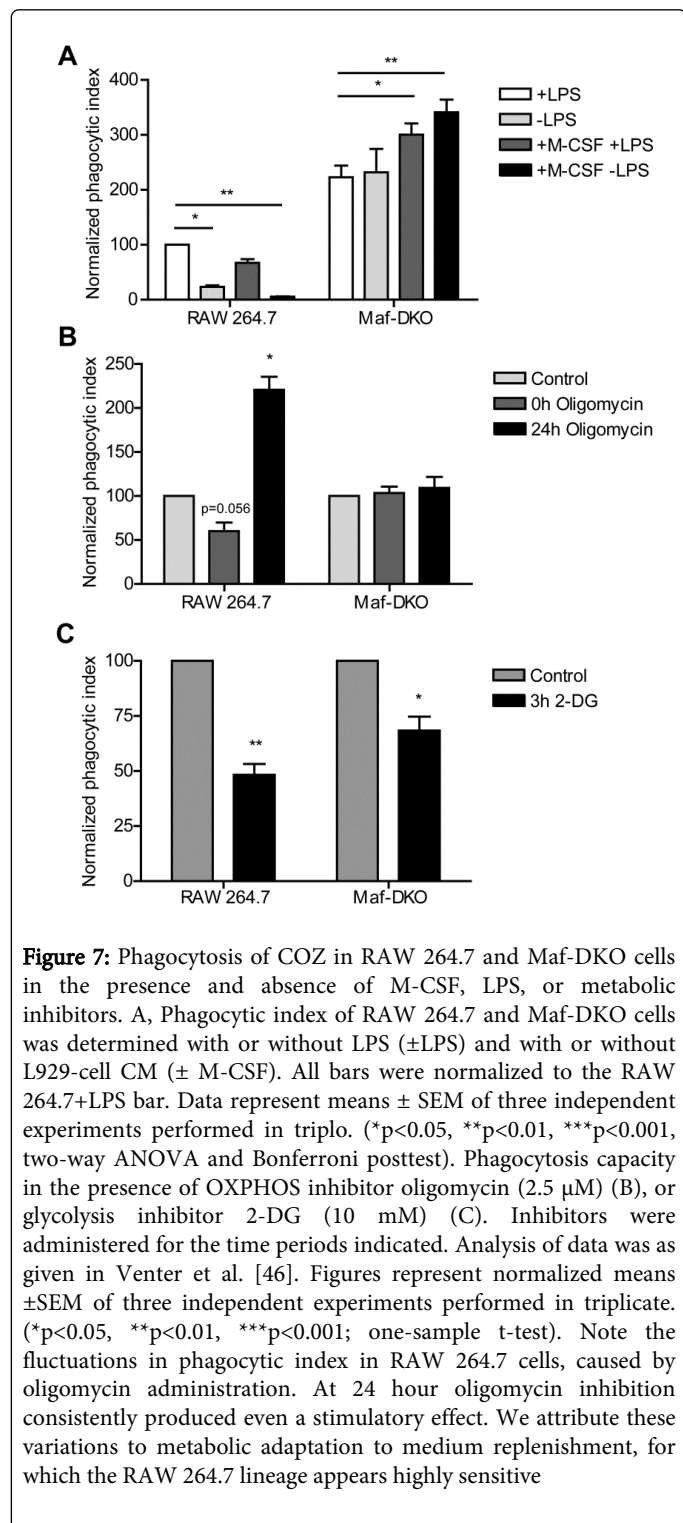


**Figure 7:** Phagocytosis of COZ in RAW 264.7 and Maf-DKO cells in the presence and absence of M-CSF, LPS, or metabolic inhibitors. A, Phagocytic index of RAW 264.7 and Maf-DKO cells was determined with or without LPS (±LPS) and with or without L929-cell CM (± M-CSF). All bars were normalized to the RAW 264.7+LPS bar. Data represent means ± SEM of three independent experiments performed in triplo. (*p<0.05, **p<0.01, ***p<0.001, two-way ANOVA and Bonferroni posttest). Phagocytosis capacity in the presence of OXPHOS inhibitor oligomycin (2.5 μM) (B), or glycolysis inhibitor 2-DG (10 mM) (C). Inhibitors were administered for the time periods indicated. Analysis of data was as given in Venter et al. [46]. Figures represent normalized means ±SEM of three independent experiments performed in triplicate. (*p<0.05, **p<0.01, ***p<0.001; one-sample t-test). Note the fluctuations in phagocytic index in RAW 264.7 cells, caused by oligomycin administration. At 24 hour oligomycin inhibition consistently produced even a stimulatory effect. We attribute these variations to metabolic adaptation to medium replenishment, for which the RAW 264.7 lineage appears highly sensitive

Phagocytic activity is a process which involves the coordination of multiple actin-based events with sudden and high energy demand. To us, our observations suggest that, although they display a marked difference in phagocytic potential, RAW 264.7 and Maf-DKO macrophages coordinate this entire process similarly in that they uniquely use fuelling by glycolysis.

In summary: Here, we have compared gross features of carbohydrate metabolism, proliferative capacity, and morphofunctional properties of Maf-DKO and RAW 264.7 macrophages, two macrophage cell lines that have an entirely different origin and history, and differentiation potential. Although there is ample evidence in literature for the existence of tight links between cellular metabolism, proliferative capacity and morphodynamic activity, we observed that both cell types share a common identity in intermediary metabolism while their behavioral properties diverge widely. While the expression levels of glycolytic enzymes and the rates of lactate production and oxygen consumption were largely similar the two cell lines exhibited vastly different proliferation rates, with the RAW 264.7 lineage having a markedly shorter doubling time, consistent with its tumorigenic origin. Maf-DKO cells, on the other hand, were morphodynamically much more active, displaying a strikingly more complex cell surface morphology and significantly greater phagocytosis efficiency. This apparent dichotomy may be best explained by assuming that, although the global rate of glycolysis in intermediary carbohydrate metabolism is similar for both cell lineages, there is differential use for this pathway. In Maf-DKO cells, its main role could be as supply pathway for ATP or metabolic intermediates to deliver fuel or cell constituents (e.g. lipids) for morphodynamic activity. In RAW 264.7 cells (aerobic) glycolysis may predominantly serve as supply pathway for associated metabolic routes for the production of precursors (nucleotides, proteins, lipids) in generation of cell biomass, or for redox protection (NADPH synthesis in the PP Pathway).

Epstein, et al. [57] have proposed that glycolysis and oxidative phosphorylation are complementary production modes that supply ATP to different cellular processes with different timescales of energy demands. In their model, cells exploit the efficiency of aerobic metabolism to meet baseline, steady-energy demand, and the rapid response time of glycolysis to meet short-timescale energy demands. By extrapolating our observations, based on the use of only two macrophage lineages of entirely different origin, we propose that the overall glycolytic phenotype might provide macrophages, irrespective of origin and specialization, with sufficient metabolic versatility and flexibility to meet with the demands that are required to fuel their vastly different immune functions. More study is necessary to better understand all details of how different aspects of carbohydrate, energy and redox metabolism are fine-tuned in accordance with growth and immune function before and after polarization and specialization of these highly plastic cell types. Clearly, also further comparative analyses are needed, but – based on our findings - we consider Maf-DKO cells that exhibit many of the typical properties of primary wild type macrophages [27], a well suited intermediate model for such studies.

## Acknowledgements

# References

1. Murray PJ, Wynn TA (2011) Protective and pathogenic functions of macrophage subsets. Nat Rev Immunol 11: 723-737.

2. Geissmann F, Manz MG, Jung S, Sieweke MH, Merad M, et al. (2010) Development of monocytes, macrophages, and dendritic cells. Science 327: 656-661.

3. Mosser DM, Edwards JP (2008) Exploring the full spectrum of macrophage activation. Nat Rev Immunol 8: 958-969.

4. van Furth R, Cohn ZA, Hirsch JG, Humphrey JH, Spector WG, et al. (1972) The mononuclear phagocyte system: a new classification of macrophages, monocytes, and their precursor cells. Bull World Health Organ 46: 845-852.

5. Davies LC, Jenkins SJ, Allen JE, Taylor PR (2013) Tissue-resident macrophages. Nat Immunol 14: 986-995.

6. Wynn TA, Chawla A, Pollard JW (2013) Macrophage biology in development, homeostasis and disease. Nature 496: 445-455.

7. Mantovani A, Sica A, Locati M (2005) Macrophage polarization comes of age. Immunity 23: 344-346.

8. Cassetta L, Cassol E, Poli G (2011) Macrophage polarization in health and disease. ScientificWorldJournal 11: 2391-2402.

9. Galli SJ, Borregaard N, Wynn TA (2011) Phenotypic and functional plasticity of cells of innate immunity: macrophages, mast cells and neutrophils. Nat Immunol 12: 1035-1044.

10. Mantovani A, Sica A, Sozzani S, Allavena P, Vecchi A, et al. (2004) The chemokine system in diverse forms of macrophage activation and polarization. Trends Immunol 25: 677-686.

11. Stout RD, Jiang C, Matta B, Tietzel I, Watkins SK, et al. (2005) Macrophages sequentially change their functional phenotype in response to changes in microenvironmental influences. J Immunol 175: 342-349.

12. Takeda N, O'Dea EL, Doedens A, Kim JW, Weidemann A, et al. (2010) Differential activation and antagonistic function of HIF-{alpha} isoforms in macrophages are essential for NO homeostasis. Genes Dev 24: 491-501.

13. Odegaard JI, Ricardo-Gonzalez RR, Goforth MH, Morel CR, Subramanian V, et al. (2007) Macrophage-specific PPARgamma controls alternative activation and improves insulin resistance. Nature 447: 1116-1120.

14. Cohen MS, Ryan JL, Root RK (1981) The oxidative metabolism of thioglycollate-elicited mouse peritoneal macrophages: the relationship between oxygen, superoxide and hydrogen peroxide and the effect of monolayer formation. J Immunol 127: 1007-1011.

15. Rodríguez-Prados JC1, Través PG, Cuenca J, Rico D, Aragonés J, et al. (2010) Substrate fate in activated macrophages: a comparison between innate, classic, and alternative activation. J Immunol 185: 605-614.

16. Roiniotis J, Dinh H, Masendycz P, Turner A, Elsegood CL, et al. (2009) Hypoxia Prolongs Monocyte/Macrophage Survival and Enhanced Glycolysis Is Associated with Their Maturation under Aerobic Conditions. J Immunol 182: 7974-7981.

17. Simon LM, Axline SG, Horn BR, Robin ED (1973) Adaptations of energy metabolism in the cultivated macrophage. J Exp Med 138: 1413-1425.

18. Bennett WE, Cohn ZA (1966) The isolation and selected properties of blood monocytes. J Exp Med 123: 145-160.

19. Vander Heiden MG, Cantley LC, Thompson CB (2009) Understanding the Warburg effect: the metabolic requirements of cell proliferation. Science 324: 1029-1033.

20. Warburg O (1956) On the origin of cancer cells. Science 123: 309-314.

21. Biswas Subhra K, Mantovani A (2012) Orchestration of Metabolism by Macrophages. Cell Metabolism 15: 432-437.

22. Haschemi A, Kosma P, Gille L, Evans Charles R, Burant Charles F, et al., (2012) The Sedoheptulose Kinase CARKL Directs Macrophage Polarization through Control of Glucose Metabolism. Cell metab 15: 813-826.

23. Davies J, Gordon S (2005) Isolation and Culture of Murine Macrophages. Methods Mol Biol 290:91-103.

24. Zhang X, Goncalves R, Mosser DM (2001) The Isolation and Characterization of Murine Macrophages. Curr Protoc Immunol Chapter 14: 1.

25. Ralph P, Prichard J, Cohn M (1975) Reticulum cell sarcoma: an effector cell in antibody-dependent cell-mediated immunity. J Immunol 114: 898-905.

26. Tsuchiya S, Yamabe M, Yamaguchi Y, Kobayashi Y, Konno T, et al. (1980) Establishment and characterization of a human acute monocytic leukemia cell line (THP-1). Int J Cancer 26: 171-176.

27. Aziz A, Soucie E, Sarrazin S, Sieweke MH (2009) MafB/c-Maf deficiency enables self-renewal of differentiated functional macrophages. Science 326: 867-871.

28. Chang EJ, Ha J, Oerlemans F, Lee YJ, Lee SW, et al. (2008) Brain-type creatine kinase has a crucial role in osteoclast-mediated bone resorption. Nat Med 14: 966-972.

29. Stanley ER, Heard PM (1977) Factors regulating macrophage production and growth. Purification and some properties of the colony stimulating factor from medium conditioned by mouse L cells. J Biol Chem 252: 4305-4312.

30. Skehan P, Storeng R, Scudiero D, Monks A, McMahon J, et al. (1990) New colorimetric cytotoxicity assay for anticancer-drug screening. J Natl Cancer Inst 82: 1107-1112.

31. Venter G, Oerlemans FT, Willemse M, Wijers M, Fransen JA, et al. (2014) NAMPT-mediated salvage synthesis of NAD+ controls morphofunctional changes of macrophages. PLoS One 9: e97378.

32. Devaraj S, Yun JM, Duncan-Staley C, Jialal I (2009) C-reactive protein induces M-CSF release and macrophage proliferation. J Leukoc Biol 85: 262-267.

33. Lee MT, Kaushansky K, Ralph P, Ladner MB (1990) Differential expression of M-CSF, G-CSF, and GM-CSF by human monocytes. J Leukoc Biol 47: 275-282.

34. Nemunaitis J (1993) Macrophage function activating cytokines: potential clinical application. Crit Rev Oncol Hematol 14: 153-171.

35. Martinez FO, Gordon S, Locati M, Mantovani A (2006) Transcriptional profiling of the human monocyte-to-macrophage differentiation and polarization: new molecules and patterns of gene expression. J Immunol 177: 7303-7311.

36. Newsholme P, Curi R, Gordon S, Newsholme EA (1986) Metabolism of glucose, glutamine, long-chain fatty acids and ketone bodies by murine macrophages. Biochem J 239: 121-125.

37. Calder PC (1995) Fuel utilization by cells of the immune system. Proc Nutr Soc 54: 65-82.

38. Dang CV, Semenza GL (1999) Oncogenic alterations of metabolism. Trends Biochem Sci 24: 68-72.

39. Mazurek S (2011) Pyruvate kinase type M2: a key regulator of the metabolic budget system in tumor cells. Int J Biochem Cell Biol 43: 969-980.

40. Brand MD, Nicholls DG (2011) Assessing mitochondrial dysfunction in cells. Biochem J 435: 297-312.

41. Valsecchi F, Monge C, Forkink M, de Groof AJ, Benard G, et al. (2012) Metabolic consequences of NDUFS4 gene deletion in immortalized mouse embryonic fibroblasts. Biochim Biophys Acta 1817: 1925-1936.

42. Yin F, Sancheti H, Cadenas E (2012) Silencing of nicotinamide nucleotide transhydrogenase impairs cellular redox homeostasis and energy metabolism in PC12 cells. Biochim Biophys Acta 1817: 401-409.

43. Bellot GL, Liu D, Pervaiz S (2013) ROS, autophagy, mitochondria and cancer: Ras, the hidden master? Mitochondrion 13: 155-162.

44. Waris G, Ahsan H (2006) Reactive oxygen species: role in the development of cancer and various chronic conditions. J Carcinog 5: 14.

45. Suzu S, Hiyoshi M, Yoshidomi Y, Harada H, Takeya M, et al. (2007) M-CSF-mediated macrophage differentiation but not proliferation is correlated with increased and prolonged ERK activation. J Cell Physiol 212: 519-525.

46. Venter G, Oerlemans FT, Wijers M, Willemse M, Fransen JA, et al. (2014) Glucose controls morphodynamics of LPS-stimulated macrophages. PLoS One 9: e96786.

47. van Horssen R, Willemse M, Haeger A, Attanasio F, Güneri T, et al. (2013) Intracellular NAD(H) levels control motility and invasion of glioma cells. Cell Mol Life Sci 70: 2175-2190.

48. Jia Z, Barbier L, Stuart H, Amraei M, Pelech S, et al. (2005) Tumor Cell Pseudopodial Protrusions: Localized signaling domains coordinating cytoskeleton remodeling, cell adhesion, glycolysis, RNA translocation, and protein translation. J Biol Chem 280: 30564-30573.

49. Brummer E, Stevens DA (1994) Effect of macrophage colony-stimulating factor (M-CSF) on macrophage morphology, phagocytosis, and intracellular multiplication of Histoplasma capsulatum. Int J Immunopharmacol 16: 171-176.

50. Kleveta G, Borzęcka K, Zdioruk M, Czerkies M, Kuberczyk H, et al. (2012) LPS induces phosphorylation of actin-regulatory proteins leading to actin reassembly and macrophage motility. J Cell Biochem 113: 80-92.

51. Williams LM, Ridley AJ (2000) Lipopolysaccharide induces actin reorganization and tyrosine phosphorylation of Pyk2 and paxillin in monocytes and macrophages. J Immunol 164: 2028-2036.

52. Aziz A, Vanhille L, Mohideen P, Kelly LM, Otto C, et al. (2006) Development of macrophages with altered actin organization in the absence of MafB. Mol Cell Biol 26: 6808-6818.

53. Roilides E, Lyman CA, Sein T, Petraitiene R, Walsh TJ (2003) Macrophage colony-stimulating factor enhances phagocytosis and oxidative burst of mononuclear phagocytes against Penicillium marneffei conidia1. FEMS Immunol Med Microbiol 36: 19-26.

54. Mitrasinovic OM, Vincent VA, Simsek D, Murphy GM Jr (2003) Macrophage colony stimulating factor promotes phagocytosis by murine microglia. Neurosci Lett 344: 185-188.

55. Patel PC, Harrison RE (2008) Membrane ruffles capture C3bi-opsonized particles in activated macrophages. Mol Biol Cell 19: 4628-4639.

56. Caron E, Self AJ, Hall A (2000) The GTPase Rap1 controls functional activation of macrophage integrin alphaMbeta2 by LPS and other inflammatory mediators. Curr Biol 10: 974-978.

57. Epstein T, Xu L, Gillies RJ, Gatenby RA (2014) Separation of metabolic supply and demand: aerobic glycolysis as a normal physiological response to fluctuating energetic demands in the membrane. Cancer Metab 2: 7.

58. von Eyben FE, Skude G, Tropé C, Wennerberg J, Mikulowski P (1982) Lactate dehydrogenase isoenzyme 1 (LDH-1) in athymic mice with xenografts of a human testicular germ cell tumor. Mol Gen Genet 186: 427-431.